International Journal of Neural Systems, Vol. 27, No. 8 (2017) 1750041 (21 pages)

DOI: 10.1142/S0129065717500411

Network Disruption in the Preclinical Stages of Alzheimer's Disease: From Subjective Cognitive Decline to Mild Cognitive Impairment

David López-Sanz
Laboratory of Cognitive and Computational Neuroscience
Center for Biomedical Technology, Complutense University of Madrid
and Technical University of Madrid 28223, Spain

Department of Basic Psychology II
Complutense University of Madrid 28223, Spain
david.lopez@ctb.upm.es

Pilar Garcés*
Laboratory of Cognitive Computational Neuroscience
Center for Biomedical Technology, Complutense University of Madrid
and Technical University of Madrid 28223, Spain
pilar.garces@ctb.upm.es

Blanca Álvarez
Memory Decline Prevention Center Madrid Salud
Ayuntamiento de Madrid 28006, Spain

María Luisa Delgado-Losada
Department of Basic Psychology II
Complutense University of Madrid 28223, Spain

Ramón López-Higes
Department of Basic Psychology II
Complutense University of Madrid 28223, Spain

Fernando Maestú
Laboratory of Cognitive and Computational Neuroscience
Center for Biomedical Technology, Complutense University of Madrid
and Technical University of Madrid 28223, Spain

Department of Basic Psychology II, Complutense University of Madrid 28223, Spain
fernando.maestu@ctb.upm.es

Accepted 8 August 2017
Published Online 29 September 2017

Introduction: Subjective Cognitive Decline (SCD) is a largely unknown state thought to represent a preclinical stage of Alzheimer's Disease (AD) previous to mild cognitive impairment (MCI). However, the course of network disruption in these stages is scarcely characterized. **Methods:** We employed resting state magnetoencephalography in the source space to calculate network smallworldness, clustering, modularity and transitivity. Nodal measures (clustering and node degree) as well as modular partitions were compared between groups. **Results:** The MCI group exhibited decreased smallworldness, clustering and transitivity and increased modularity in theta and beta bands. SCD showed similar but smaller changes in clustering and transitivity, while exhibiting alterations in the alpha band in opposite direction to those showed by MCI for modularity and transitivity. At the node level, MCI disrupted both clustering and nodal degree while SCD showed minor changes in the latter. Additionally, we observed an increase in

*Corresponding author.

modular partition variability in both SCD and MCI in theta and beta bands. **Conclusion:** SCD elders exhibit a significant network disruption, showing intermediate values between HC and MCI groups in multiple parameters. These results highlight the relevance of cognitive concerns in the clinical setting and suggest that network disorganization in AD could start in the preclinical stages before the onset of cognitive symptoms.

Keywords: Alzheimer's disease; subjective cognitive decline; mild cognitive impairment; network; magnetoencephalography.

1. Introduction

Alzheimer's Disease (AD) is the most common cause of dementia.[1] It is an insidious and neurodegenerative disease that produces a progressive decline in multiple cognitive domains, especially episodic memory.[2] There is a growing interest in the preclinical stages of the disease due to the lack of a curative treatment[3] and the dramatic increase expected in the number of cases in the future.[4]

AD is considered as a disconnection syndrome.[5] Accordingly, many studies have revealed a progressive loss of functional connectivity (FC) between key brain regions in AD patients.[6,7] For this reason, a network perspective is suitable to characterize the specific patterns of alterations affecting the connections between different brain regions in the AD continuum. Given the large amount of data derived from this kind of analyzes, graph theory has become a very powerful tool in neuroimaging to summarize and study the organization of whole brain networks and capture the alterations in the network structure caused by the disease.[8] Graph theory describes a network as a set of nodes, the components of a system (represented in the brain network perspective as a region of interest-(ROI)), and a number of edges, representing the connection between each pair of nodes.[9,10]

The brain exhibits a particular organization characterized by a large number of short-range connections between related areas while maintaining some long range connections between less related areas. This *small-world* topology[11] is especially suited for cognitive processing[12] and is the expression of a trade-off between the pressure to minimize wiring cost (i.e. reducing long range axons) and maximizing information flow and integration.[13] Alzheimer's causes major disruption in network organization, affecting not only this small-world architecture of the brain[14,15] but also other brain network properties like clustering or modularity.[16]

Graph theory can help us unravel the degenerative process occurring during the extended preclinical phase of AD, which could start over 15 years before the onset of clinical symptoms.[17] Mild cognitive impairment (MCI) is a well-known at-risk stage of AD, characterized by a slight although detectable cognitive decline in one or more cognitive domains.[18] MCI patients exhibit multiple evidences of AD pathology such as cortical atrophy,[19] β-amyloid depositions[20] or connectivity disruption.[21] This brain pathology translates into network alterations similar to those exhibited by AD patients.[22,23]

Earlier in the course of the disease, healthy elders with normal neuropsychological performance could manifest a subjective feeling of cognitive worsening. The inclusion of this stage, coined as subjective cognitive decline (SCD),[24] in the preclinical asymptomatic stage of AD still remains a matter of debate.[25] Although some studies did not find evidences of AD pathology in the brain of SCD elders,[26,27] there is a growing body of literature supporting the link between cognitive concerns and characteristic AD signs such as β-amyloid accumulation,[28] reduction of glucose metabolism in AD related areas[29] and relative power decreases in alpha band[30] among others. Furthermore, a meta-analysis combining data from more than 29,000 subjects has revealed that healthy elders with SCD are twice as likely to develop dementia than individuals without cognitive concerns.[31] The conversion rate to AD for SCD is even greater when segregating healthy elders with positive β-amyloid into SCD and non-SCD.[32] However, very little is known about the beginning of network disruption in this stage. The only study to date addressing this issue employed structural networks to build graph matrices, reporting no differences between healthy elders with and without cognitive concerns.[33] Although from a theoretical perspective graph metrics provide a common framework that allows comparison between networks coming from

different types of data,[23] evidence suggests that differences in methodology and relatively small sample sizes may produce divergent results.[16]

To the best of our knowledge, this is the first study to date employing graph metrics built from functional data to characterize the evolution of network dynamics throughout the preclinical stages of AD including healthy elders without cognitive concerns (HC), healthy elders with SCD, and MCI patients. To this aim, we employed resting state activity recorded with magnetoencephalography (MEG) and reconstructed source level activity to precisely detect and localize changes in brain network properties and modular organization. Electrophysiological measures of synchrony derived from EEG or MEG have been proven useful in the detection of different pathologies[34–36] and specifically in AD.[37,38] Based on previous imaging studies, we expected to detect altered network properties in MCI patients with respect to HC. More importantly, we hypothesized that SCD elders will show alterations in the same direction of those exhibited by MCI patients, although to a lower extent, thus exhibiting intermediate values between HC and MCI.

2. Methods

2.1. *Subjects*

The sample for this study was recruited from two recent projects funded by the Spanish Ministry of Economy and Competitiveness. In total, 187 elders were included in this study recruited from three centers: the neurology department at "Hospital Clínico San Carlos", the "Center for cognitive impairment prevention" and the "Seniors center of Chamartín District", all of them in Madrid, Spain. Participants were divided into three groups: 63 healthy elders with neuropsychological performance within the normal range and no subjective feeling of cognitive decline (HC), 55 healthy elders with unimpaired cognitive performance but with SCD and 69 elders with Mild Cognitive Impairment (MCI). Subjects were aged between 60 and 81 years old. Table 1 summarizes relevant clinical and demographic data. The exclusion criteria to enroll in the study included the following: (1) history of psychiatric or neurological disorders or drug consumption that could affect MEG activity such as cholinesterase inhibitors, (2) evidence of infection, infarction or focal lesions in a T2-weighted scan within 2 months before MEG acquisition (3) a modified Hachinski score equal to 5 or higher, (4) a GDS-SF score equal to 5 or higher, (5) alcoholism, chronic use of anxiolytics, neuroleptics, narcotics, anticonvulsants or sedative hypnotics. Furthermore, we conducted additional analysis to rule out other possible causes of cognitive decline such as B12 vitamin deficit, diabetes mellitus, thyroid problems, syphilis, or Human Immunodeficiency Virus (HIV).

All participants signed an informed consent. This study was approved by the Clínico San Carlos Hospital ethics committee and the procedure was performed in accordance with approved guidelines and regulations.

2.2. *Clinical assessment*

An initial screening was carried out to assess the general functioning and cognitive status of the sample. This screening included The Mini Mental State Examination (MMSE),[39] the Hachinski Ischemic Score (HIS),[40] the Functional Assessment Questionnaire (FAQ)[41] and the Geriatric Depression Scale — Short Form (GDS-SF).[42] Each of the participants underwent an extensive neuropsychological assessment, whereupon in the following weeks they completed a magnetic resonance imaging (MRI) scanner and a MEG scan. The neuropsychological assessment included: Direct and Inverse Digit Span Test (Wechsler Memory Scale, WMS-III), Immediate and Delayed Recall (WMS-III), Phonemic and Semantic Fluency (Controlled oral Word Association Test, COWAT), Ideomotor Praxis of Barcelona Test, Boston Naming Test (BNT) and Trail Making Test A and B (TMTa and TMTb) and Rule Shift Cards (Behavioral Assessment of the Dysexecutive Syndrome, BADS).

MCI diagnosis was carried out according to the criteria established by Petersen[43] and Grundman.[44] In addition, MCI subjects did not fulfill criteria for dementia diagnosis.

All the participants included into the HC or SCD group showed a normal cognitive performance in the neuropsychological tests. Information regarding cognitive concerns was collected during an interview with clinician experts, where subjects self-reported whether they felt a significant cognitive decline with respect to their previous performance

Table 1. The left half of the table shown mean ± SD (standard deviation). The right half of the table shown the p-values resulting of the significant between groups ANOVA comparisons. If the factor is not significant a hyphen is shown. If a specific *post hoc* comparison is not significant ($\alpha = 0.05$) 'n.s.' is shown. Education was measured from 1 (illiterate) to 5 (university studies).

	Mean ± SD			p-values		
	Control	SCD	MCI	HC-SCD	HC-MCI	SCD-MCI
Age (years)	70.7 ± 4.5	71 ± 5	71.9 ± 4.2	—	—	—
Gender (M/F)	24/39	13/42	22/47	—	—	—
GDS	1.4 ± 1.84	1.8 ± 1.7	3.8 ± 3.2	n.s.	4.5×10^{-8}	6.3×10^{-6}
Education	4.19 ± 1	3.95 ± 1	3 ± 1.15	n.s.	1.4×10^{-9}	2.7×10^{-6}
MMSE	28.9 ± 1.2	29 ± 1	26.8 ± 2.4	n.s.	9.7×10^{-10}	9.6×10^{-10}
Dir. digits	8.5 ± 1.9	8.7 ± 2	7.3 ± 2.2	n.s.	0.004	0.0003
Inv. digits	6.2 ± 1.9	5.6 ± 2	4.3 ± 1.5	n.s.	3.3×10^{-9}	0.0002
TMTb hits	23.2 ± 2.6	22.4 ± 3.2	19.4 ± 6.1	n.s.	3.5×10^{-6}	5.2×10^{-4}
TMTb time (s)	108.7 ± 60.8	133 ± 62	227.6 ± 102.6	n.s.	9.5×10^{-10}	1.2×10^{-9}
Imm. recall	41.7 ± 11	34.8 ± 11	18.3 ± 7.4	0.0005	9.5×10^{-10}	9.5×10^{-10}
Del. recall	25.1 ± 8	20.4 ± 8.6	7.5 ± 6.2	0.001	9.5×10^{-10}	9.5×10^{-10}
Hipp. volume	0.005 ± 5.10^{-4}	0.005 ± 6.10^{-4}	0.004 ± 8.10^{-4}	n.s.	2×10^{-6}	2×10^{-5}

Note: ODS stands for Geriatric Depression Scale - Short Form. MMSE stands for Mini Mental State Examination, Dir. digits and inv. digits stand for direct and inverse digit span test respectively. TMTb stands for Trail Making Test form b. Imm. Recall and del. recall stand for immediate and delayed recall of the WMS-III, respectively. Hipp. Volume stands for normalized hippocampal volume.

level. The final group assignment was made by multidisciplinary consensus (neuropsychologists, psychiatrists and neurologists). Several possible confounders of SCD such as: medication, psycho-affective disorders or relevant medical conditions were taken into account for the decision. According to the SCD International Working Group (SCD-I-WG), all the participants were older than 60 at onset of SCD, which occurred within the last five years.[24]

2.3. *MRI acquisition*

A T1-weighted MRI was available for each subject, acquired in a General Electric 1.5 Tesla magnetic resonance scanner, using a high-resolution antenna and a homogenization PURE filter (Fast Spoiled Gradient Echo sequence, TR/TE/TI = 11.2/4.2/450 ms; flip angle 12°; 1 mm slice thickness, 256×256 matrix and FOV 25 cm). MRI images were processed with Freesurfer software (version 5.1.0) and its specialized tool for automated cortical and subcortical segmentation[45] in order to obtain the volume of both hippocampi. The volume of both hippocampi was averaged and then normalized dividing it by the total intracranial volume to account for head volume differences between subjects.

2.4. *MEG recordings and preprocessing*

Electrophysiological data were acquired by using a 306 channel (102 magnetometers, 204 planar gradiometers) Vectorview MEG system (Elekta AB, Stockholm, Sweden), placed inside a magnetically shielded room (VacuumSchmelze GmbH, Hanau, Germany) at the "Laboratory of Cognitive and Computational Neuroscience" (Madrid, Spain). All recordings were obtained while subjects were sitting comfortably, resting awake with eyes closed. MEG acquisition consisted of four minutes of signal for each subject. During the recording continuous information of the head position, blinks and eye movements were acquired.

MEG data was registered using a sampling rate of 1000 Hz and an online anti-aliasing bandpass filter between 0.1 Hz and 330 Hz. Recordings were processed offline using a spatiotemporal signal space separation algorithm with movement compensation[46] (correlation window 0.9, time window 10 s) in order to remove magnetic noise originated outside the head.

We employed an automatic procedure from Fieldtrip package to detect ocular, muscular and jump artifacts,[47] and the artifact detection was visually

confirmed by a MEG expert afterwards. The remaining data were segmented in 4 seconds epochs of artefact-free activity. Additionally, an ICA-based procedure was employed to remove the electrocardiographic component. Due to the redundancy between gradiometers and magnetometers after temporal-signal space separation (tSSS) filtering, only magnetometers were used for further analysis.

2.5. *Source reconstruction*

The source model consisted of 2459 sources placed in a homogeneous grid of 1 cm in the Montreal Neurological Institute (MNI) template, then linearly transformed to subject space. The leadfield was calculated using a three-shell Boundary Element Method (brain-skull, skull-scalp and scalp-air interfaces generated from the subject's T1 MRI) computed with OpenMEEG software.[48]

MEG data were band-pass filtered in theta (4–8 Hz), alpha (8–12 Hz) and beta (12–30 Hz) bands using an 1800 order finite input response (FIR) filter designed using Hanning window. Our frequency band choice was based on previous studies reporting greater reliability of graph metrics in these specific bands.[49–51] Data was filtered in a two-pass procedure as implemented in Matlab's filtfilt to avoid phase distortion. 2000 samples of real data at each side were employed as padding to avoid edge effects. Linearly Constrained Minimum Variance (LCMV) beamformer[52] was employed to solve the inverse problem and calculate source time-series.

2.6. *Functional connectivity calculation*

First, source time series for 52 regions of interest (ROIs) were extracted using a data-driven functional atlas created by Craddock *et al.*.[53] The original atlas consisted of 60 ROIs extracted through spatially constrained spectral clustering, generating spatially coherent regions of homogeneous resting state FC. For our MEG analysis, only cortical ROIs were employed, resulting in 52 total ROIs. The activity of each ROI was defined as the time series of the source within the ROI which showed the highest correlation with all its neighbors in the ROIs.

For each frequency band, the functional coupling between each pair of ROIs was estimated with envelope correlation with leakage correction.[54,55] First, pairwise ROI time series were orthogonalized through a linear regression between both signals. The orthogonalization solves the problem of the artifactual correlations generated by the ill-posed inverse problem, thus avoiding bias in FC estimates due to source leakage. Afterwards, the envelopes of the two orthogonalized time-series were calculated with the modulus of the Hilbert transform of the ROI time series, already band-pass filtered in the specific frequency band. The FC between any two ROIs was estimated as the Pearson correlation coefficient between their envelopes. Since the orthogonalization of the time series is nonsymmetrical, the final FC estimate between two ROIs was defined as the average of the envelope correlation values obtained when using both ROI time series as seeds separately.[56]

2.7. *Graph calculations*

In general, a graph (G) is expressed as a set of nodes (V) and the connections between those nodes, or edges (E); $G = (V, E)$. The connections between nodes are stored in a weight matrix (W). In this matrix, the weight (w) of the connection between the node i and the node j is captured by the element w_{ij} of the graph. When constructing weighted networks in neuroimaging, weak connections represent a major limitation in graph analysis because they may introduce spurious correlations into the matrix, adding noise into the network.[23] Consequently, we employed a binarized version of the original connection matrix of each subject using an arbitrary threshold (τ). Any connection with a value below the selected threshold was set to zero, those values higher than the threshold were set to one. $w_{ij} < \tau = 0; w_{ij} \geq \tau = 1$. AD and MCI patients are known to exhibit lower FC values.[57–59] As a consequence, their binarized matrices when employing a given FC threshold could be sparser than those of HC, which is known to significantly affect graph metrics.[14] In fact, MCI patients showed a decreased matrix density in the beta band (and both SCD and MCI showed a trend towards sparser networks in the theta band) when using a given FC value to threshold all the matrices. To avoid this effect we selected a critical value for each individual FC matrix such that the proportion of edges overpassing this threshold was set to a fixed percentage, or matrix density. Choosing a specific threshold

involves an arbitrary decision, therefore, according to Rubinov and Sporns[9] it is considered good practice to explore changes in network topology across a wide range of matrix densities to ensure robustness of results. We set our threshold range from 5% to 35% of matrix edges to ensure quality and completeness of the data.[60] Similar ranges have been commonly employed in the literature according to Bassett and Bullmore.[12] To enable comparison between groups, we created a surrogate distribution of network parameters for each frequency band and subject and normalized all value parameters by subtracting the mean surrogate value and dividing it by the surrogate standard deviation. Networks constructed using correlation show higher clustering values than random networks given the transitive nature of correlation. Thus, it is important to use random networks that preserve these features characteristic of correlational networks. We employed the Hirschberger-Qi-Steuer (HQS) algorithm,[61] implemented for FC matrices in Ref. 62, which maintains the mean and variance of the off-diagonal elements and the mean of the diagonal elements of the FC matrix.

2.8. *Network parameters*

All network and nodal parameters were calculated using a freely available toolbox for Matlab: Brain Connectivity Toolbox.[9]

2.8.1. *Small-world* (S)

Brain networks are thought to reconcile a large amount of short range connections for segregation while maintaining a sufficient amount of long range connections to ensure processing integration. The small-world parameter of a binarized network is defined as the ratio between normalized clustering coefficient (C_{glob}) and normalized path length (L) with respect to a null model network.[63] And thus represents the ratio between the amount of short range connectivity (or segregation) and the distance between any two nodes, i.e. network integration. The random networks for small-world calculation were generated using HQS algorithm, given the tendency of correlational networks to overestimate smallworldness if an inappropriate null model is employed.

$$S = \frac{C_{\text{glob}}/C_{\text{rand}}}{L/L_{\text{rand}}}. \tag{1}$$

2.8.2. *Global clustering coefficient* (C_{glob})

Clustering coefficient is a measure of local connectivity representing the fraction of triangles surrounding a node. It was implemented in BCT as defined in Ref. 11. That is to say, the algorithm calculates how many of the nodes to which a node is connected, are also connected between them. C_{glob} is defined as the mean clustering of all nodes. The mean clustering coefficient is then normalized individually for each node, thus being possibly biased by the presence of nodes with a low degree. This is the clustering definition employed:

$$C_i = \frac{2E_i}{k_i(k_i - 1)}, \tag{2}$$

where C_i is the clustering of each node which is averaged afterwards to obtain C_{glob}, E_i is the number of edges between the neighbors of i and k_i is the degree of node i, i.e. the number of neighbors the node has.

2.8.3. *Transitivity* (T)

Transitivity, similarly to clustering, reflects how well a node is connected to its neighboring areas. However, unlike clustering coefficient, transitivity is quite robust against the presence of barely connected nodes. Instead of being normalized individually for each node, transitivity is normalized by the value of the whole network,[64] thus being more resistant to the presence of nodes with low degree. Transitivity was calculated following the definition in Ref. 65;

$$T = \frac{3 \cdot \text{number of triangles}}{\text{number of paths of length } 2'}, \tag{3}$$

where a triangle is a set of three nodes in which each is linked by an edge with the other two.

2.8.4. *Modularity* (Q)

The optimal modular partition is a subdivision of the network that is able to maximize the ratio between intra-module edges versus inter-module edges.[66] Q parameter is a statistic representing how well the partition of the current network fits that definition. We calculated modularity as the average Q through 100 runs considering that the value on each run may slightly vary due to heuristics in the algorithm. Q value was calculated according to Newman's formula[66] by subtracting the expected number of edges in a given community from the actual number

of such edges. In a particular division of a network larger Q values indicate stronger community structure.

2.9. *Nodal parameters*

To best localize and define topological changes in the network we studied the alterations shown by MCI and SCD at the nodal level in three key parameters. For the sake of brevity, all the results at the nodal level correspond to an intermediate matrix density. (i.e. 15%), although several other thresholds were inspected to ensure the consistency of the results across different matrix densities.

2.9.1. *Local clustering coefficient* (C_{loc})

To further characterize differences in local connectedness in both groups we studied variations in clustering patterns across all 52 ROIs between groups with the above-mentioned clustering definition. However, instead of averaging the clustering coefficients across our 52 nodes, we inspected the clustering for each node separately.

2.9.2. *Degree* (D)

The degree is a measure reflecting the importance of a node in a network. It is calculated by counting the number of suprathreshold links in which a node is involved after binarization of the correlation matrix, that is to say, the number of neighbors a node has after thresholding.

2.9.3. *Modular structure*

Differences in modular structure were studied comparing partition assignments at the nodal level between groups. To this aim we calculated for each subject 1000 partitions and then selected the most representative subdivision of the network for each subject.[67] After that, we employed the same procedure to choose the most representative partition for each group from the partitions of their members. In each step, we first calculated an agreement matrix with the n initial partitions ($n = 1000$ for each subject in the first step, and n = number of subjects in each group in the second step). This matrix contained the probability for each two nodes of the network of being included in the same module. After that, we employed the algorithm as described in Ref. 67 to find a consensus partition of the agreement matrix. This algorithm partitions the agreement matrix a number of times to then extract a single representative agreement partition.

2.10. *Statistics*

We used ANCOVA with age as covariate to test group differences in all the network parameters ($\alpha = 0.05$). Besides, considering that MCI patients had a lower educational level, we repeated all the analyses with education as a covariate and ensured that our results were not driven by this variable as all the effects reported remained unchanged. In the case of nodal degree and clustering, p-values were corrected using False Discovery Rate for each specific comparison[68] ($Q = 0.2$). To test differences in modular distribution at the node level, we calculated differences between each pair of partitions by means of their distance as an information theoretic measure as implemented in Ref. 69. This procedure quantifies the normalized variation of information between partitions applying the equation:

$$VI_n = \frac{H(x) + H(Y) - 2 \cdot MI(X,Y)}{\log(n)}, \qquad (4)$$

where H is the entropy of each partition, MI is mutual information and n is the number of nodes. X and Y correspond to each of the modular partitions compared. Intra-group and inter-group distances were compared to test for differences in modular structure between groups. Afterwards, we compared the intra-group variability of the individual partitions across groups with a Wilkoxon test.

We conducted correlation analyses using Pearson coefficient in our whole sample between our network parameters: (small-world, clustering, transitivity, modularity and individual partition distance to their group's standard partition) and a subset of neuropsychological tests, one belonging to each of the cognitive domains mainly affected in early AD: memory with the "immediate recall test" from the Wechsler Memory Scale, and executive functions with the TMTb time. We also included MMSE as an indicator of overall cognitive status. With this analysis we aimed to study the relationship between network disruption and cognitive status. P-values for the correlations were also FDR corrected.

3. Results

3.1. *Network results*

3.1.1. *Small-world* (S)

Regarding small-world (Fig. 1), all three groups exhibited small-world like brain network topologies with values over 1 for all matrix densities. MCI patients showed a decrease in most of the thresholds with respect to HC in the theta (p-range = 0.0001–0.044) and beta band (p-range = 0.00001–0.037). MCI also exhibited a decrease in S compared to SCD in theta (p-range 0.02–0.045) and beta bands (p-range = 0.01–0.047). However, differences between MCI and SCD were significant for a fewer number of thresholds. There were no significant differences in small-world topology between HC and SCD groups.

3.1.2. *Clustering* (C_{glob})

MCI and SCD elders exhibited a decrease in global network clustering in theta and beta bands with respect to HC. SCD clustering values were intermediate between HC and MCI (Fig. 1). More concretely, network clustering in MCI patients was decreased compared to HC in the theta (p-range = 0.0004–0.037) and beta band (p-range = 0.00003–0.049). There were no differences in clustering coefficient between MCI and SCD in theta or alpha band. Significant differences between these two groups were found only for two matrix densities in the beta band (p-range = 0.027–0.036). However given that these results are very sparse across thresholds they should be cautiously interpreted, as they could reflect an arbitrary effect due to the specific thresholding value. Similarly to MCI, SCD elders showed a decrease in the clustering coefficient with respect to HC in theta (p-range 0.018–0.04) and beta bands (p-range 0.015–0.045). However, these differences were evident in a smaller number of thresholds in both frequency bands.

3.1.3. *Modularity* (Q)

MCI patients exhibited increases in modularity in theta band when compared to HC (p-range = 0.001–0.049) and SCD (p-range = 0.022–0.041), although the latter comparison involved only three significant matrix densities. In this case differences between MCI and SCD should be carefully interpreted given that SCD showed intermediate modularity values between HC and MCI in this matrix density range (Fig. 1). In the alpha band SCD network modularity was decreased compared to both HC (p-range = 0.022–0.048) and MCI (p-range = 0.022–0.048). Regarding beta band, an increase in modularity was observed in MCI patients with respect to HC (p-range = 0.009–0.044) and SCD (p-range = 0.015–0.037).

3.1.4. *Transitivity* (T)

In the theta band, we observed a progressive decrease in transitivity from HC to SCD and then MCI (Fig. 1). Concretely, SCD transitivity value was significantly lower compared to HC in a few thresholds (p-range = 0.042–0.048), but still higher than MCI for every matrix density (p-range = 0.013–0.045). It is important to take into account that even though SCD transitivity in this frequency band showed an intermediate decrease between HC and MCI, the statistical significance was not robust across thresholds, so this result should be carefully interpreted. MCI transitivity was also decreased with respect to the HC group (p-range = $8 \cdot 10^{-6}$–0.0001). Network transitivity was increased in SCD elders in the alpha band with respect to both HC group (p-range = 0.016–0.048) and MCI patients (p-range = 0.0009–0.005). Regarding beta band, MCI patients exhibited a decrease in transitivity with respect to SCD (p-range = 0.005–0.044), and a more consistent decrease across thresholds when compared to HC group (p-range = 0.0004–0.03).

3.2. *Node results*

3.2.1. *Local clustering changes*

As shown in Fig. 2, we observed alterations in clustering coefficient in the MCI group when compared to HC at the node level. In the theta band, these alterations involved clustering decreases specially located in posterior areas and lateral areas such as left middle temporal lobe, both inferior parietal lobes, and right superior occipital regions. Two frontal nodes also exhibited a decrease in clustering in this frequency band in MCI patients. Regarding beta band, we observed a posterior decrease in nodal clustering in MCI patients affecting inferior and middle temporal lobe and right lingual gyrus. However,

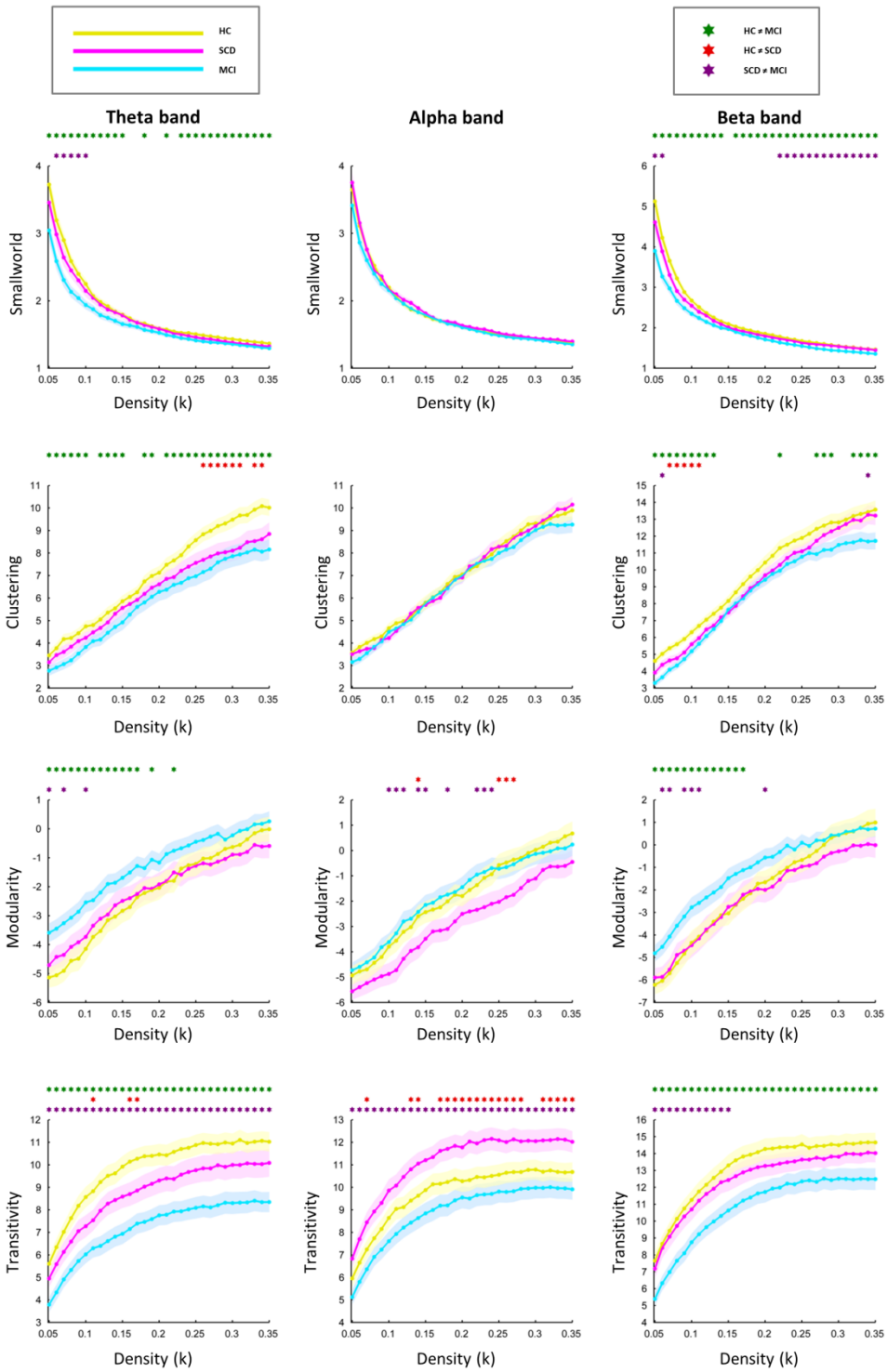

Fig. 1. Mean network parameters for each diagnostic group as a function of matrix density (k). Shaded areas represent mean standard error. If the difference between two groups for a given matrix density is significant ($\alpha = 0.05$), an asterisk with the specific color code of that comparison is shown in the upper part of each graph. Each row shows the results for a different network parameter: small-world, clustering, modularity and transitivity, respectively. Each column corresponds to a specific frequency band: theta, alfa and beta band, respectively.

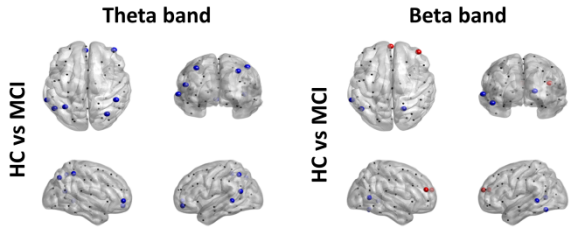

Fig. 2. (Color online) Figure displays significant nodal clustering differences between groups. Blue spheres indicate a decrease in the specific node in MCI group. Red spheres indicate an increase in the specific node in MCI group.

we found an increase in clustering coefficient in the frontal lobe in both; right superior medial and left middle frontal lobe. Interestingly, SCD clustering levels seem to be in an intermediate state between HC and MCI as we found no differences between HC and SCD nor between SCD and MCI.

3.2.2. *Local degree changes*

Our results showed alterations in nodal degree both in SCD and MCI, although the latter showed disruptions over much broader regions (Fig. 3). With respect to the HC group, MCI patients exhibited a clearly divided dual pattern of posterior degree decreases and anterior increases in theta and beta band. Posterior nodes affected by this degree decrease involved bilateral occipital, middle temporal lobe and parietal areas including two nodes located in the left precuneus. Regions with increased nodal degree included bilateral middle and superior frontal gyrus, left hippocampus, anterior cingulate cortex and the insula among others. SCD elders also exhibited a nodal degree increase in left postcentral node with respect to HC in the beta band

The comparison between SCD and MCI revealed similar results in the theta band, where MCI patients demonstrated lower degree values over posterior brain regions and degree increases in anterior nodes of the network. Similar regions were affected in the theta band in both comparisons (HC versus MCI and SCD verus MCI) although a smaller number of nodes showed degree abnormalities in the latter. Furthermore, in the alpha band one node located in the left superior occipital lobe showed a significant decrease in degree in the MCI group with respect to SCD. Interestingly, no differences were found between SCD

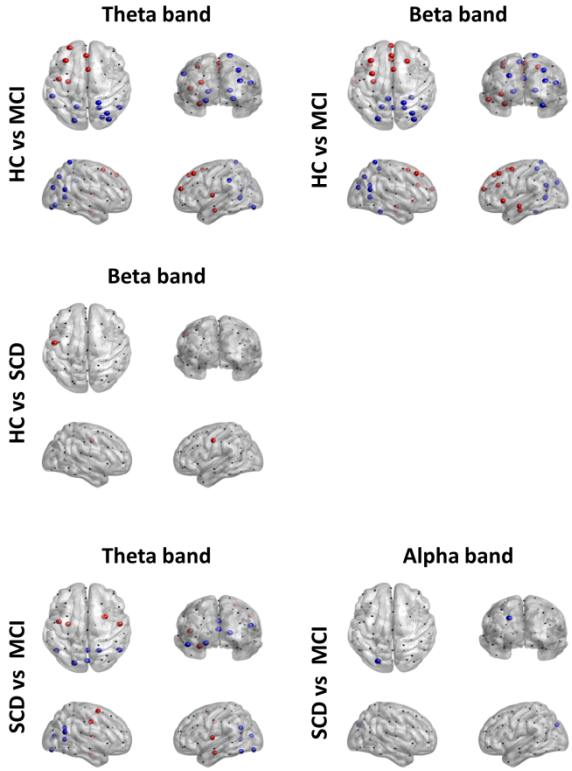

Fig. 3. (Color online) Figure displays significant nodal degree differences between groups. Blue spheres indicate a degree decrease in the group in a more advanced stage of the disease (i.e. MCI < HC, SCD < HC and MCI < SCD respectively). On the contrary, red spheres indicate degree increases in this group (i.e. MCI > HC, SCD > HC and MCI > SCD, respectively).

and MCI in the beta band, in which MCI exhibited larger alterations with respect to the HC group.

3.2.3. *Modular distribution*

We did not observe significant modular distribution changes between groups in any of the contrasts ($\alpha = 0.05$). That is to say, between-groups partitions distance was not significantly larger than the intra-group partitions distance. Given that we did not observe significant modular changes between groups only HC module partitions are shown in Fig. 4.

To further investigate modular distribution properties in each group, we studied in more detail the intra-group variability, comparing within-group partition distances across diagnostics i.e. the distance between modular partitions of each possible pair of participants in each group. Interestingly, we observed a highly significant linear increase in the intra-group

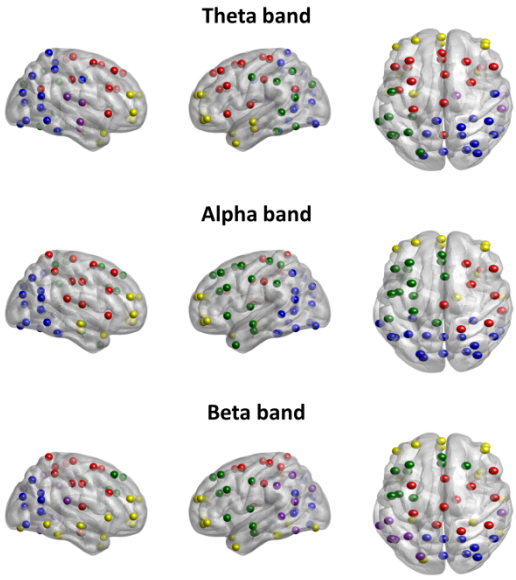

Fig. 4. (Color online) Figure displays modular partitions for HC group in in theta, alpha and beta band, respectively. The color of each sphere indicates that node belongs to a specific brain module.

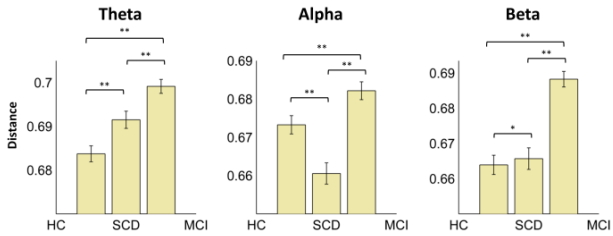

Fig. 5. Figure displays the mean distance between module distributions of each pair of participants in each group in theta, alpha and beta bands (left to right, respectively) and the standard error of the mean for each bar. *Notes*: * stands for $p < 0.05$. ** stands for $p < 0.001$.

modular variability with advancing pathology in the theta and beta band (Fig. 5). Specifically, in the theta band MCI patients showed more variability than HC ($p < 0.001$) and SCD ($p < 0.001$). Furthermore, SCD modular partitions variability between subjects was also larger compared to HC ($p < 0.001$). Similarly, in the beta band, MCI showed the largest between subjects distances, with respect to both HC ($p < 0.001$) and SCD ($p < 0.001$). SCD variability was also larger compared to HC ($p = 0.014$). Lastly, MCI patients also presented larger intra-group distances in the alpha band than SCD ($p < 0.001$) and HC ($p < 0.001$). On the contrary, we did not observe a linear increase in this specific frequency range as SCD elders demonstrated lower between-subject distances than the HC group ($p < 0.001$).

3.3. *Hippocampal volume*

We compared hippocampal volume extracted from the MRI T1 images in our sample. We used an ANCOVA with diagnostic as the main factor and age as covariate. A significant main effect was found for diagnosis ($p < 10^{-6}$). *Post hoc* comparisons revealed that MCI normalized hippocampal volume was significantly smaller compared to both HC ($p < 10^{-5}$) and SCD ($p < 10^{-4}$). Interestingly HC and SCD did not show any differences in their hippocampal volume ($\alpha = 0.05$).

3.4. *Correlations*

To help interpret the meaning of the disruptions found in SCD and MCI groups, we conducted a series of correlations in our sample. The complete set of significant correlations after FDR correction is listed in Table 2. Regarding network parameters, we observed that in the theta, and beta bands, the disruptions observed in SCD and MCI correlated with a worst cognitive state. More specifically, decreases in theta or beta band in small-world or transitivity, and increases in modularity were associated with a poorer performance in neuropsychological assessment. Additionally, in the alpha band, a decrease in modularity and an increase in transitivity were associated to a higher MMSE score. No significant correlations were found between cognitive performance and clustering coefficient.

Lastly, in order to better characterize the changes demonstrated by SCD and MCI in the intra-group variability of their modular distributions, we conducted a series of correlations. For each subject, we obtained the distance between his own modular partition, and the representative partition of his group. Afterwards, we correlated that distances with neuropsychological tests. In the beta band, we observed that the more different a subject's modular distribution was from his group, the worst his performance was in memory, executive functions and his general cognitive state. In the alpha band, where SCD showed a decrease in intra-group variability, we observed a similar pattern; those subjects with similar partitions to its group were able to complete

Table 2. Significant correlations and their p-value after FDR correction between cognitive tests and network parameters for each frequency band.

		THETA BAND		ALPHA BAND		BETA BAND	
Network	Cognition	rho	p-value	rho	p-value	rho	p-value
Small-World	Imm. recall	—	—	—	—	0.2	0.005
	TMTb time	—	—	—	—	−0.19	0.01
Modularity	MMSE	—	—	−0.16	0.03	—	—
	Imm. recall	—	—	—	—	−0.22	0.003
Transitivity	MMSE	0.19	0.009	0.14	0.04	—	—
	Imm. recall	0.2	0.007	—	—	0.31	2×10^{-5}
	TMTb time	−0.17	0.03	—	—	−0.2	0.009
Partition deviation	MMSE	—	—	—	—	−0.15	0.03
	Imm. recall	—	—	—	—	−0.25	5.5×10^{-4}
	TMTb	—	—	0.18	0.01	0.23	0.002

TMTb faster than those with more different modular distribution.

4. Discussion

In the present work, we found several alterations in the network organization of MCI and SCD elders. Elders with MCI exhibited decreased small-world, clustering and transitivity and increased modularity. Furthermore, we observed disruptions in the degree distribution of their nodes and in their nodal clustering. Lastly, the variability of their modular distributions was significantly increased, thus exhibiting great disparity between subject's partitions. However, the most striking and novel finding is the presence of alterations in several network parameters in healthy elders with SCD, such as clustering, transitivity, modularity and the changes observed in intragroup partitions' heterogeneity. More importantly, despite the fact that these disruptions were less pronounced in SCD, the majority of these changes were in line with those found in MCI. SCD showed intermediate values between HC and MCI groups in multiple network parameters. This is the first study reporting network disruption in SCD elders. To the best of our knowledge, the only study to date studying network topology in SCD reported preserved white matter organization in SCD.[33] Interestingly, in their study SCD elders also exhibited intermediate network parameter values between HC and MCI. The larger sample size of our study probably allowed us to detect significant differences accounting for the discrepancies in the results. Our findings support the notion of SCD as an asymptomatic at-risk state of AD, suggesting an AD-continuum starting several years before clinical manifestations appearance in the MCI stage.

At the network level, we observed several alterations in the different parameters estimated in both MCI, and SCD. Interestingly, most of these disruptions were found only for the theta and beta bands, and not in the alpha range, which is the predominant resting state rhythm. This could suggest that network structure in the alpha band is relatively preserved until later in the course of the disease.

A loss of small-world like architecture has been traditionally associated with AD[70,71] and it has also been documented in MCI patients.[22] In our data, the reduction observed in small-world affected only MCI group in theta and beta bands. This decrease in small-world is thought to impair normal brain organization. Furthermore, MCI networks are known to be less efficient and slower in information flow,[72] which is consistent with a decrease in smallworldness. Smallworld-like networks combine a high number of short range connections at a low cost, with some long range connections maintaining an efficient information flow between distant brain regions.[73] This specific network disorganization present in AD has been related with alterations in regions with a critical role for information flow, the so-called hubs,[15] which are known to be affected in the early stages of the disease.[16] However, small-world architecture seems to be preserved in the SCD stage.

Clustering and transitivity parameters reflect how well the different regions of the brain are connected into their own local cluster. Even though

studies reporting transitivity are yet scarce, previous results suggest that it is a superior method to study AD-like networks.[22] As a consequence, we calculated both parameters to ensure similar results and compare with the previous literature, which mainly used clustering coefficient in AD. Overall, we observed decreases in local connectedness in MCI and SCD, especially affecting theta and beta bands. There are no previous studies reporting decreased clustering coefficient in SCD. However, a reduction in network clustering has been reported with different methods such as functional magnetic resonance imaging (fMRI) in AD[16,74] or cortical thickness and volume with MRI in MCI patients[22] who also exhibited transitivity reductions in this study. MCI and AD patients also showed clustering reductions in a previous study using sparse inverse covariance estimation with positron emission tomography (PET)[75] which seems to be an optimal and reliable methodology for studying AD.[76] Thus, our results for SCD and MCI are consistent with the previous literature. The increase in transitivity in the alpha band showed by SCD elders reflects an increase in the number of short-range connections in this specific frequency range. Interestingly, we observed that those subjects with higher transitivity values in the alpha band demonstrated an overall better cognitive status. Although still tentative, this result could suggest a compensatory mechanism underpinning the normal cognitive performance of SCD elders in spite of their abnormal clustering in other frequency bands.

Regarding modularity, we again observed a similar pattern in theta and beta bands. MCI patients exhibited increased modularity in those bands with respect to both HC and SCD. Modularity is thought to represent the functional organization of the brain, and its value is large when the nodes of each module are strongly connected to their relatives and weakly connected to other modules. Our results are consistent with the previous studies reporting an increase in modularity in MCI and AD patients[22] and also in Parkinson's Disease patients with MCI at risk of developing dementia.[77] However, there are also inconsistent results, and some studies reported decreased modularity in AD.[16] Our finding points to a worse communication between different functional modules, thus decreasing the ability of the different network components to share information and work together. This inefficient communication between brain modules has been previously linked with worse cognitive performance in AD patients.[78] Interestingly, in our results-higher modularity scores in the beta band were related to worse memory performance in immediate recall, and in the previous studies, they were also associated with memory and visuospatial ability impairment.[77] These findings highlight the pathological nature of modularity alterations. In the alpha band, SCD elders were the only group showing alterations, a significant reduction in modularity. Lower modularity in the alpha band was associated with a more preserved cognitive state, suggesting again a possible compensatory mechanism. Furthermore, a previous study found that increases in task demand were associated with reductions in the modularization of brain networks.[79] This effect was interpreted as an attempt to increase long-distance synchronization between different functional systems to overcome cognitive demands. In fact, those subjects with lower modularity values performed faster. These findings seem to support the compensatory interpretation of the alpha band results in SCD elders.

After studying network disruption in the preclinical stages of AD we aimed to localize changes within the brain. We first compared the degree distribution across brain regions between the three different groups. AD is known to affect the hub-like behavior of crucial nodes of the network,[16] but very little is known about the preclinical asymptomatic stage of the disease. In our analysis, MCI patients exhibited nodal degree decreases over critical areas of the posterior default mode network (DMN) such as precuneus, parietal and middle temporal structures in the theta and beta bands when compared to HC. AD is a disconnection syndrome known to reduce functional connectivity over posterior brain regions.[7,80] Interestingly, this connectivity alterations in the brain match with the spatiotemporal distribution pattern of Alzheimer's pathophysiology.[6] In addition, we observed increases in node degree over anterior regions including frontal areas, temporal structures and a central hub of the anterior DMN; the anterior cingulate cortex. These findings reinforce previous work reporting disrupted nodal strength in posterior and temporal regions of the brain, and increases over anterior areas,[81–83] and expand them to the preclinical stages of the disease. Besides, these results are compatible with previous

work from our group reporting a dual pattern change in the FC profile of both MCI and SCD showing anterior hypersynchronization and FC reduction over similar posterior brain regions.[84] Interestingly, we did not find in the present work such a pattern in the nodal degree of SCD group, which could indicate that even though significant synchronization alterations are already present in this group, degree distribution seems to be still relatively preserved compared to MCI patients. Furthermore, SCD group exhibited increased nodal strength in a postcentral node in the theta band. Using graph theory approaches, degree increases of certain nodes have also been associated with a greater node vulnerability in different contexts such as World Wide Web, metabolic or social networks.[85] Interestingly, SCD group did not show any significant difference in the beta band when compared either to HC or MCI, thus showing intermediate values between both states.

Regarding nodal clustering changes, it is worth noting that the only differences were found between HC and MCI. SCD local clustering was different neither from HC nor from MCI group. This raises the idea that SCD is situated in a somewhat intermediate state between both conditions hindering the identification of significant differences. MCI elders exhibited widespread clustering decreases indicative of local disconnection in those nodes. This is consistent with previous works in MCI's structural networks.[22] Furthermore, in the beta band, we found both clustering decreases located in posterior regions and nodes exhibiting increased clustering coefficient over frontal areas. This shift in local connectedness from posterior to anterior areas has been found mostly for high frequency bands, which could explain the different pattern obtained for theta and beta bands.[82]

Regarding functional networks organization, we lastly compared the different modular partitions of the three diagnostic groups. Modular structure of the brain has been repeatedly associated with cognitive performance,[78,79,86] thus becoming a relevant network feature to characterize the preclinical stages of AD. We did not observe a consistent reorganization in preclinical AD networks. However, we observed (specifically for theta and beta bands) an increasing variability between subjects' modular partitions with advancing pathology, thus, in average, differences between each pair of modular partitions of SCD or MCI patients were larger than in the HC group. These findings could point towards pathological modular structure disorganization. It is worth noting that in all three bands, those subjects whose modular partition were farther from their representative group partition, performed worse in memory, executive functioning and overall cognitive state as measured by MMSE. Although modular reorganization in AD has been reported previously,[22,78] small sample sizes and the use of merely descriptive methods (rather than statistical comparison) may explain divergent results. Particularly, taking into account the apparent increased variability in AD network organization, sample size seems to be a crucial factor to make modular comparisons robust and reliable.

We also included a brief analysis of gray matter integrity in a key structure in AD progression, the hippocampus. As expected, according to multiple previous studies,[19,87] MCI patients showed signs of atrophy over medial temporal regions. However, it is of note that we did not observe any sign of hippocampal atrophy in the SCD group as they showed almost identical levels of hippocampal volume compared to HC. The results to this regard are quite inconsistent in the literature, while some studies found a significant deterioration in this region,[88] others reported no signs of gray matter loss.[89] While hippocampal volume represents a useful tool in the later stages of the disease, as it has proven to correctly classify MCI and AD patients,[90] it is relevant to highlight that according to our results, MEG is able to capture subtle alterations in network organization even before standard MRI volumetric analysis is able to detect them as reflected in our results.

This study reinforces the idea of SCD as a preclinical asymptomatic stage of AD. While still preserving some intact network features, SCD elders evidenced disruptions at the network level compatible with those exhibited by MCI patients, although to a lower extent. Interestingly, SCD group showed changes in transitivity and modularity in the alpha band in opposite direction to those exhibited by MCI patients, which could be interpreted as a compensatory mechanism. These findings are in line with previous studies reporting intermediate but detectable pathological levels in healthy elders presenting cognitive concerns in different modalities such as MEG power spectra,[30] gray matter atrophy[91,92] or β-amyloid accumulation in AD-related

areas.[93,94] Furthermore, previous studies found that β-amyloid accumulation could reach a plateau before the onset of AD.[95] Consequently, it is a likely hypothesis that those SCD elders that will eventually develop AD show some accumulation at this stage already, thus disrupting to some extent their network behavior. More research is needed to expand and replicate the knowledge of this preclinical stage. However, these results highlight the relevance of cognitive concerns in the clinical setting and point towards a continuum in the prodromic stages of the disease from healthy control to MCI or AD through the SCD stage.

4.1. *Limitations and future directions*

This study has two main limitations. On the one hand, some of the network differences reported should be cautiously interpreted as mentioned before, namely, differences between SCD and MCI in beta band clustering or theta band modularity, or those in theta band transitivity between HC and SCD are restricted to only a few thresholds, thus limiting the robustness of those results. This problem is inherently related with the second major limitation of this study, the fact that SCD is a quite heterogeneous entity, thus increasing the variability of our results. Even though there are multiple evidences reporting SCD elders are at an increased risk for developing AD and MCI[24,31] and show increased levels of AD pathology,[92,96] the present study is cross-sectional and the exact fraction of the SCD cohort that will go on to develop AD is unknown. Our current definitions and limited understanding of SCD hamper our ability to discriminate those individuals with AD pathology from those that will not develop the disease. Future next steps should involve Computer Aided Diagnosis (CAD) in the SCD stage. Previous work has used CAD on AD and MCI with either MRI,[97–99] or MEG[100,101] successfully classifying and diagnosing at an individual level, for a review, see Ref. 102. However, its use applied to earlier stages is very limited nowadays. A refinement in SCD selection criteria is needed to allow employing such procedures to study the evolution of this at risk of AD population.

Author contributions

DLS conducted MEG recordings; DLS and PG carried out data analysis; DLS and PG wrote the paper; DLS prepared the figures; BA, MLD and RLH recruited the sample and carried out neuropsychological assessment; FM and RLH designed the experiment. All the authors read and corrected the paper.

Acknowledgments

This study was supported by two projects from the Spanish Ministry of Economy and Competitiveness, PSI2009-14415-C03-01 and PSI2012-38375-C03-01, and a predoctoral fellowship from the Ministry of Economy and Competitiveness to DLS (PSI2012-38375-C03-01).

References

1. K. Blennow, M. J. de Leon and H. Zetterberg, Alzheimer's disease, *Lancet* **368** (2006) 387–403, doi:10.1016/S0140-6736(06)69113-7.
2. J. Peña-Casanova, G. Sánchez-Benavides, S. de Sola, R. M. Manero-Borrás and M. Casals-Coll, Neuropsychology of Alzheimer's Disease, *Arch. Med. Res.* **43** (2012) 686–693, doi:10.1016/j.arcmed.2012.08.015.
3. K. Iqbal, F. Liu and C.-X. Gong, Alzheimer disease therapeutics: focus on the disease and not just plaques and tangles, *Biochem. Pharmacol.* **88** (2014) 631–639, doi: 10.1016/j.bcp.2014.01.002.
4. C. P. Ferri, M. Prince, C. Brayne, H. Brodaty, L. Fratiglioni, M. Ganguli, K. Hall, K. Hasegawa, H. Hendrie, Y. Huang, A. Jorm, C. Mathers, P. R. Menezes, E. Rimmer and M. Scazufca, Global prevalence of dementia: a Delphi consensus study, *Lancet* **366** (2005) 2112–2117, doi:10.1016/S0140-6736(05)67889-0.
5. X. Delbeuck, M. Van der Linden and F. Collette, Alzheimer' Disease as a Disconnection Syndrome?, *Neuropsychol. Rev.* **13** (2003) 79–92, doi:10.1023/A:1023832305702.
6. D. Jones, D. S. Knopman, J. L. Gunter, J. Graff-Radford, P. Vemuri, B. F. Boeve, R. C. Petersen, M. W. Weiner and C. R. Jack, Cascading network failure across the Alzheimer's disease spectrum, *Brain.* **139** (2015) 547–562, doi:10.1093/brain/awv338.
7. J. S. Damoiseaux, K. E. Prater, B. L. Miller and M. D. Greicius, Functional connectivity tracks clinical deterioration in Alzheimer's disease, *Neurobiol. Aging.* **33** (2012) 828.e19-828.e30, doi:10.1016/j.neurobiolaging.2011.06.024.
8. M. Filippi, M. P. van den Heuvel, A. Fornito, Y. He, H. E. Hulshoff Pol, F. Agosta, G. Comi and M. A. Rocca, Assessment of system dysfunction in the brain through MRI-based connectomics, *Lancet Neurol.* **12** (2013) 1189–1199, doi:10.1016/S1474-4422(13)70144-3.

9. M. Rubinov and O. Sporns, Complex network measures of brain connectivity: Uses and interpretations, *Neuroimage.* **52** (2010) 1059–1069, doi:10.1016/j.neuroimage.2009.10.003.
10. O. Sporns, D. Chialvo, M. Kaiser and C. Hilgetag, Organization, development and function of complex brain networks, *Trends Cogn. Sci.* **8** (2004) 418–425, doi:10.1016/j.tics.2004.07.008.
11. D. J. Watts and S. H. H. Strogatz, Collective dynamics of "small-world" networks, *Nature.* **393** (1999) 440–442, doi:10.1038/30918.
12. D. S. Bassett and E. T. Bullmore, Small-world brain networks revisited. *The Neuroscientist* (2016), doi:10.1177/1073858416667720.
13. E. Bullmore and O. Sporns, The economy of brain network organization, *Nat. Rev. Neurosci.* **13** (2012) 336, doi:10.1038/nrn3214.
14. E. J. Sanz-Arigita, M. M. Schoonheim, J. S. Damoiseaux, S. A. R. B. Rombouts, E. Maris, F. Barkhof, P. Scheltens and C. J. Stam, Loss of "Small-World" Networks in Alzheimer's Disease: Graph Analysis of fMRI Resting-State Functional Connectivity, *PLoS One* **5** (2010) e13788, doi:10.1371/journal.pone.0013788.
15. C. J. Stam, W. de Haan, A. Daffertshofer, B. F. Jones, I. Manshanden, A. M. van Cappellen van Walsum, T. Montez, J. P. A. Verbunt, J. C. de Munck, B. W. van Dijk, H. W. Berendse and P. Scheltens, Graph theoretical analysis of magnetoencephalographic functional connectivity in Alzheimer's disease, *Brain* **132** (2008) 213–224, doi:10.1093/brain/awn262.
16. M. R. Brier, J. B. Thomas, A. M. Fagan, J. Hassenstab, D. M. Holtzman, T. L. Benzinger, J. C. Morris and B. M. Ances, Functional connectivity and graph theory in preclinical Alzheimer's disease, *Neurobiol. Aging* **35** (2014) 757–768, doi:10.1016/j.neurobiolaging.2013.10.081.
17. C. R. Jack, D. S. Knopman, W. J. Jagust, R. C. Petersen, M. W. Weiner, P. S. Aisen, L. M. Shaw, P. Vemuri, H. J. Wiste, S. D. Weigand, T. G. Lesnick, V. S. Pankratz, M. C. Donohue and J. Q. Trojanowski, Tracking pathophysiological processes in Alzheimer's disease: an updated hypothetical model of dynamic biomarkers, *Lancet Neurol.* **12** (2013) 207–216, doi:10.1016/S1474-4422(12)70291-0.
18. R. C. Petersen, Mild Cognitive Impairment., *Continuum Minneap. Minn.* **22** (2016) 404–418, doi:10.1212/CON.0000000000000313.
19. X. Ma, Z. Li, B. Jing, H. Liu, D. Li and H. Li, Alzheimer's Disease Neuroimaging Initiative, Identify the Atrophy of Alzheimer's Disease, Mild Cognitive Impairment and Normal Aging Using Morphometric MRI Analysis, *Front. Aging Neurosci.* **8** (2016) 243, doi:10.3389/fnagi.2016.00243.
20. E. C. Edmonds, K. J. Bangen, L. Delano-Wood, D. A. Nation, A. J. Furst, D. P. Salmon and M. W. Bondi, Alzheimer's Disease Neuroimaging Initiative, Patterns of Cortical and Subcortical Amyloid Burden across Stages of Preclinical Alzheimer's Disease, *J. Int. Neuropsychol. Soc.* **22** (2016) 978–990, doi:10.1017/S1355617716000928.
21. F. Maestú, J.-M. Peña, P. Garcés, S. González, R. Bajo, A. Bagic, P. Cuesta, M. Funke, J. P. Mäkelä, E. Menasalvas, A. Nakamura, L. Parkkonen, M. E. López, F. del Pozo, G. Sudre, E. Zamrini, E. Pekkonen, R. N. Henson and J. T. Becker, Magnetoencephalography International Consortium of Alzheimer's Disease, A multicenter study of the early detection of synaptic dysfunction in Mild Cognitive Impairment using Magnetoencephalography-derived functional connectivity, *NeuroImage Clin.* **9** (2015) 103–109, doi:10.1016/j.nicl.2015.07.011.
22. J. B. Pereira, M. Mijalkov, E. Kakaei, P. Mecocci, B. Vellas, M. Tsolaki, I. Kłoszewska, H. Soininen, C. Spenger, S. Lovestone, A. Simmons, L. O. Wahlund, G. Volpe and E. Westman, Disrupted Network Topology in Patients with Stable and Progressive Mild Cognitive Impairment and Alzheimer's Disease, *Cereb. Cortex.* **26** (2016) 3476–3493, doi:10.1093/cercor/bhw128.
23. B. M. Tijms, A. M. Wink, W. de Haan, W. M. van der Flier, C. J. Stam, P. Scheltens and F. Barkhof, Alzheimer's disease: connecting findings from graph theoretical studies of brain networks, *Neurobiol. Aging.* **34** (2013) 2023–2036, doi:10.1016/j.neurobiolaging.2013.02.020.
24. F. Jessen, R. E. Amariglio, M. van Boxtel, M. Breteler, M. Ceccaldi, G. Chételat, B. Dubois, C. Dufouil, K. A. Ellis, W. M. van der Flier, L. Glodzik, A. C. van Harten, M. J. de Leon, P. McHugh, M. M. Mielke, J. L. Molinuevo, L. Mosconi, R. S. Osorio, A. Perrotin, R. C. Petersen, L. A. Rabin, L. Rami, B. Reisberg, D. M. Rentz, P. S. Sachdev, V. de la Sayette, A. J. Saykin, P. Scheltens, M. B. Shulman, M. J. Slavin, R. A. Sperling, R. Stewart, O. Uspenskaya, B. Vellas, P. J. Visser and M. Wagner, A conceptual framework for research on subjective cognitive decline in preclinical Alzheimer's disease, *Alzheimer's Dement* **10** (2014) 844–852, doi:10.1016/j.jalz.2014.01.001.
25. S. Röhr, T. Luck, A. Villringer, M. C. Angermeyer, S. G. Riedel-Heller, Subjektiver kognitiver Abbau und Demenzentwicklung — Ergebnisse der Leipziger Langzeitstudie in der Altenbevökerung (LEILA75+), *Psychiatr. Prax.* **44** (2017) 47–49, doi:10.1055/s-0042-118593.
26. C. C. Rowe, K. A. Ellis, M. Rimajova, P. Bourgeat, K. E. Pike, G. Jones, J. Fripp, H. Tochon-Danguy, L. Morandeau, G. O'Keefe, R. Price, P. Raniga, P. Robins, O. Acosta, N. Lenzo, C. Szoeke, O. Salvado, R. Head, R. Martins, C. L. Masters, D. Ames and V. L. Villemagne, Amyloid imaging results from the Australian Imaging, Biomarkers

and Lifestyle (AIBL) study of aging, *Neurobiol. Aging* **31** (2010) 1275–1283, doi:10.1016/j.neurobiolaging.2010.04.007.

27. R. Buckley, M. M. Saling, D. Ames, C. C. Rowe, N. T. Lautenschlager, S. L. Macaulay, R. N. Martins, C. L. Masters, T. O'Meara, G. Savage, C. Szoeke, V. L. Villemagne and K. A. Ellis, Factors affecting subjective memory complaints in the AIBL aging study: biomarkers, memory, affect, and age, *Int. Psychogeriatr* **25** (2013) 1307–1315, doi:10.1017/S1041610213000665.
28. M. M. Mielke, H. J. Wiste, S. D. Weigand, D. S. Knopman, V. J. Lowe, R. O. Roberts, Y. E. Geda, D. M. Swenson-Dravis, B. F. Boeve, M. L. Senjem, P. Vemuri, R. C. Petersen and C. R. Jack, Indicators of amyloid burden in a population-based study of cognitively normal elderly, *Neurology* **79** (2012) 1570–1577, doi:10.1212/WNL.0b013e31826e2696.
29. L. Scheef, A. Spottke, M. Daerr, A. Joe, N. Striepens, H. Kölsch, J. Popp, M. Daamen, D. Gorris, M. T. Heneka, H. Boecker, H. J. Biersack, W. Maier, H. H. Schild, M. Wagner and F. Jessen, Glucose metabolism, gray matter structure, and memory decline in subjective memory impairment, *Neurology* **79** (2012) 1332–1339, doi:10.1212/WNL.0b013e31826c1a8d.
30. D. López-Sanz, R. Bruña, P. Garcés, C. Camara, N. Serrano, I. C. Rodríguez-Rojo, M. L. Delgado, M. Montenegro, R. López-Higes, M. Yus and F. Maestú, Alpha band disruption in the AD-continuum starts in the Subjective Cognitive Decline stage: a MEG study, *Sci. Rep.* **6** (2016) 37685, doi:10.1038/srep37685.
31. A. J. Mitchell, H. Beaumont, D. Ferguson, M. Yadegarfar and B. Stubbs, Risk of dementia and mild cognitive impairment in older people with subjective memory complaints: meta-analysis, *Acta Psychiatr. Scand.* **130** (2014) 439–451, doi:10.1111/acps.12336.
32. R. F. Buckley, P. Maruff, D. Ames, P. Bourgeat, R. N. Martins, C. L. Masters, S. Rainey-Smith, N. Lautenschlager, C. C. Rowe, G. Savage, V. L. Villemagne and K. A. Ellis, Subjective memory decline predicts greater rates of clinical progression in preclinical Alzheimer's disease, *Alzheimer's Dement.* **12** (2016) 796–804, doi:10.1016/j.jalz.2015.12.013.
33. X.-N. N. Wang, Y. Zeng, G.-Q. Q. Chen, Y.-H. H. Zhang, X.-Y. Y. Li, X.-Y. Y. Hao, Y. Yu, M. Zhang, C. Sheng, Y.-X. X. Li, Y. Sun, H.-Y. Li, Y. Song, K.-C. Li, T.-Y. Yan, X.-Y. Tang, Y. Han, Abnormal organization of white matter networks in patients with subjective cognitive decline and mild cognitive impairment, *Oncotarget.* **7** (2016) 552, doi:10.18632/oncotarget.10601.
34. R. Coullaut-Vallera, I. Arbaiza, R. Bajo, R. Arrue, M. E. López, J. Coullaut-Vallera, A. Correas, D. López-Sanz, F. Maestú and D. Papo, Drug polyconsumption is associated with increased synchronization of brain electrical activity at rest and in a counting task, *Int. J. Neural Syst.* **24** (2014) 1450005, doi:10.1142/S0129065714500051.
35. A. Correas, S. Rodriguez Holguín, P. Cuesta, E. López-Caneda, L. M. García-Moreno, F. Cadaveira and F. Maestú, Exploratory Analysis of Power Spectrum and Functional Connectivity During Resting State in Young Binge Drinkers: A MEG Study, *Int. J. Neural Syst.* **25** (2015) 1550008, doi:10.1142/S0129065715500082.
36. D. Chyzhyk, M. Graña, D. Öngür and A. K. Shinn, Discrimination of schizophrenia auditory hallucinators by machine learning of resting-state functional MRI, *Int. J. Neural Syst.* **25** (2015) 1550007, doi:10.1142/S0129065715500070.
37. N. Houmani, G. Dreyfus and F. B. Vialatte, Epoch-based Entropy for Early Screening of Alzheimer's Disease, *Int. J. Neural Syst.* **25** (2015) 1550032, doi:10.1142/S012906571550032X.
38. M. Ahmadlou, H. Adeli and A. Adeli, New diagnostic EEG markers of the Alzheimer's disease using visibility graph, *J. Neural Transm.* **117** (2010) 1099–1109, doi:10.1007/s00702-010-0450-3.
39. A. Lobo, J. Ezquerra, F. Gómez Burgada, J. M. Sala and A. Seva Díaz, [Cognocitive mini-test (a simple practical test to detect intellectual changes in medical patients)], *Actas luso-españolas Neurol. Psiquiatr. y ciencias afines.* **7** (1979) 189–202, http://europepmc.org/abstract/med/474231 (accessed on 29 January, 2016).
40. W. G. Rosen, R. D. Terry, P. A. Fuld, R. Katzman and A. Peck, Pathological verification of ischemic score in differentiation of dementias, *Ann. Neurol.* **7** (1980) 486–488, doi:10.1002/ana.410070516.
41. R. I. Pfeffer, T. T. Kurosaki, C. H. Harrah, J. M. Chance and S. Filos, Measurement of Functional Activities in Older Adults in the Community, *J. Gerontol.* **37** (1982) 323–329, doi:10.1093/geronj/37.3.323.
42. J. A. Yesavage, T. L. Brink, T. L. Rose, O. Lum, V. Huang, M. Adey and V. O. Leirer, Development and validation of a geriatric depression screening scale: A preliminary report, *J. Psychiatr. Res.* **17** (1982) 37–49, doi:10.1016/0022-3956(82)90033-4.
43. R. C. Petersen, Mild cognitive impairment as a diagnostic entity., *J. Intern. Med.* **256** (2004) 183–94, doi:10.1111/j.1365-2796.2004.01388.x.
44. M. Grundman, Mild Cognitive Impairment Can Be Distinguished From Alzheimer Disease and Normal Aging for Clinical Trials, *Arch. Neurol.* **61** (2004) 59, doi:10.1001/archneur.61.1.59.
45. B. Fischl, D. H. Salat, E. Busa, M. Albert, M. Dieterich, C. Haselgrove, A. van der Kouwe, R. Killiany, D. Kennedy, S. Klaveness, A. Montillo, N. Makris, B. Rosen and A. M. Dale, Whole brain segmentation: automated labeling of neuroanatomical structures in the human brain, *Neuron*

33 (2002) 341–355, http://www.ncbi.nlm.nih.gov/pubmed/11832223 (accessed on 6 January, 2015).
46. S. Taulu and J. Simola, Spatiotemporal signal space separation method for rejecting nearby interference in MEG measurements, *Phys. Med. Biol.* **51** (2006) 1759–1768, doi:10.1088/0031-9155/51/7/008.
47. R. Oostenveld, P. Fries, E. Maris and J.-M. Schoffelen, FieldTrip: Open source software for advanced analysis of MEG, EEG, and invasive electrophysiological data, *Comput. Intell. Neurosci.* **2011** (2011) 156869, doi:10.1155/2011/156869.
48. A. Gramfort, T. Papadopoulo, E. Olivi and M. Clerc, OpenMEEG: opensource software for quasistatic bioelectromagnetics, *Biomed. Eng. Online* **9** (2010) 45, doi:10.1186/1475-925X-9-45.
49. M. Hardmeier, F. Hatz, H. Bousleiman, C. Schindler, C. J. Stam and P. Fuhr, Reproducibility of functional connectivity and graph measures based on the phase lag index (PLI) and weighted phase lag index (wPLI) derived from high resolution EEG, *PLoS One* **9** (2014) e108648, doi:10.1371/journal.pone.0108648.
50. L. Deuker, E. T. Bullmore, M. Smith, S. Christensen, P. J. Nathan, B. Rockstroh and D. S. Bassett, Reproducibility of graph metrics of human brain functional networks, *Neuroimage* **47** (2009) 1460–1468, doi:10.1016/j.neuroimage.2009.05.035.
51. S.-H. Jin, J. Seol, J. S. Kim and C. K. Chung, How reliable are the functional connectivity networks of MEG in resting states?, *J. Neurophysiol.* **106** (2011) 2888–2895, doi:10.1152/jn.00335.2011.
52. B. D. Van Veen, W. van Drongelen, M. Yuchtman and A. Suzuki, Localization of brain electrical activity via linearly constrained minimum variance spatial filtering, *IEEE Trans. Biomed. Eng.* **44** (1997) 867–880, doi:10.1109/10.623056.
53. R. C. Craddock, G. A. James, P. E. Holtzheimer, X. P. Hu and H. S. Mayberg, A whole brain fMRI atlas generated via spatially constrained spectral clustering, *Hum. Brain Mapp.* **33** (2012) 1914–1928, doi:10.1002/hbm.21333.
54. M. J. Brookes, M. W. Woolrich and G. R. Barnes, Measuring functional connectivity in MEG: A multivariate approach insensitive to linear source leakage, *Neuroimage* **63** (2012) 910–920, doi:10.1016/j.neuroimage.2012.03.048.
55. J. F. Hipp, D. J. Hawellek, M. Corbetta, M. Siegel and A. K. Engel, Large-scale cortical correlation structure of spontaneous oscillatory activity, *Nat. Neurosci.* **15** (2012) 884–890, doi:10.1038/nn.3101.
56. G. L. Colclough, M. J. Brookes, S. M. Smith and M. W. Woolrich, A symmetric multivariate leakage correction for MEG connectomes, *Neuroimage* **117** (2015) 439–448, doi:10.1016/j.neuroimage.2015.03.071.
57. M. R. Brier, J. B. Thomas, A. Z. Snyder, T. L. Benzinger, D. Zhang, M. E. Raichle, D. M. Holtzman, J. C. Morris and B. M. Ances, Loss of intranetwork and internetwork resting state functional connections with Alzheimer's disease progression., *J. Neurosci.* **32** (2012) 8890–8899, doi:10.1523/JNEUROSCI.5698-11.2012.
58. J. Wang, X. Zuo, Z. Dai, M. Xia, Z. Zhao, X. Zhao, J. Jia, Y. Han and Y. He, Disrupted functional brain connectome in individuals at risk for Alzheimer's disease, *Biol. Psychiatry.* **73** (2013) 472–481, doi:10.1016/j.biopsych.2012.03.026.
59. Z. Sankari, H. Adeli and A. Adeli, Wavelet Coherence Model for Diagnosis of Alzheimer Disease, *Clin. EEG Neurosci.* **43** (2012) 268–278, doi:10.1177/1550059412444970.
60. D. S. Bassett and E. Bullmore, Small-World Brain Networks, *Neuroscience* **12** (2006) 512–523, doi:10.1177/1073858406293182.
61. M. Hirschberger, Y. Qi and R. E. Steuer, Randomly generating portfolio-selection covariance matrices with specified distributional characteristics, *Eur. J. Oper. Res.* **177** (2007) 1610–1625, doi:10.1016/j.ejor.2005.10.014.
62. A. Zalesky, A. Fornito and E. Bullmore, On the use of correlation as a measure of network connectivity, *Neuroimage* **60** (2012) 2096–2106, doi:10.1016/j.neuroimage.2012.02.001.
63. M. D. Humphries, K. Gurney and T. J. Prescott, The brainstem reticular formation is a small-world, not scale-free, network, *Proc. Biol. Sci.* **273** (2006) 503–511, doi:10.1098/rspb.2005.3354.
64. M. E. J. Newman, The Structure and Function of Complex Networks, *SIAM Rev.* **45** (2003) 167–256, doi:10.1137/S003614450342480.
65. M. D. Humphries and K. Gurney, Network "small-world-ness": A quantitative method for determining canonical network equivalence, *PLoS One* **3** (2008) e0002051. doi:10.1371/journal.pone.0002051.
66. M. E. J. Newman, Finding community structure in networks using the eigenvectors of matrices, Phys. Rev. E - Stat. Nonlinear, *Soft Matter Phys.* **74** (2006) 36104, doi:10.1103/PhysRevE.74.036104.
67. A. Lancichinetti and S. Fortunato, Consensus clustering in complex networks, *Sci. Rep.* **2** (2012) 336, doi:10.1038/srep00336.
68. Y. Benjamini, Y. Hochberg, Y. Benjamini and Y. Hochberg, Controlling the false discovery rate: a practical and powerful approach to multiple testing, *J. R. Stat. Soc. B.* **57** (1995) 289–300, doi:10.2307/2346101.
69. M. Meilă, Comparing clusterings—an information based distance, *J. Multivar. Anal.* **98** (2007) 873–895, doi:10.1016/j.jmva.2006.11.013.
70. F. C. Morabito, M. Campolo, D. Labate, G. Morabito, L. Bonanno, A. Bramanti, S. de Salvo, A. Marra and P. Bramanti, A Longitudinal EEG Study of Alzheimer's Disease Progression Based on A Complex Network Approach, *Int. J. Neural Syst.* **25** (2015) 1550005, doi:10.1142/S0129065715500057.

71. E. J. Sanz-Arigita, M. M. Schoonheim, J. S. Damoiseaux, S. A. R. B. Rombouts, E. Maris, F. Barkhof, P. Scheltens, C. J. Stam, X. Delbeuck, M. Van der Linden, F. Collette, M. O'Sullivan, D. Jones, P. Summers, R. Morris, S. Williams, M. Greicius, B. Krasnow, A. Reiss, V. Menon, M. Raichle, A. MacLeod, A. Snyder, W. Powers, D. Gusnard, R. Desimone, J. Duncan, J. Hopfinger, M. Buonocore, G. Mangun, J. Damoiseaux, C. Beckmann, E. S. Arigita, C. Stam, F. Barkhof, M. Greicius, G. Srivastava, A. Reiss, V. Menon, K. Wang, M. Liang, L. Wang, L. Tian, X. Zhang, I. Mason, J. Damoiseaux, C. Beckmann, E. Arigita, F. Barkhof, P. Scheltens, C. Grady, D. Hongwanishkul, M. Keightley, W. Lee, L. Hasher, J. Lindeboom, H. Weinstein, C. Grady, A. McIntosh, S. Beig, M. Keightley, H. Burian, C. Sole-Padulles, D. Bartres-Faz, C. Junque, P. Vendrell, L. Rami, J. Woodard, S. Grafton, J. Votaw, R. Green, M. Dobraski, K. Supekar, V. Menon, D. Rubin, M. Musen, M. Greicius, C. Stam, B. Jones, G. Nolte, M. Breakspear, P. Scheltens, Y. He, Z. Chen, A. Evans, J. Reijneveld, S. Ponten, H. Berendse, C. Stam, S. Strogatz, C. Stam, B. Van Dijk, D. Watts, S. Strogatz, P. Hagmann, M. Kurant, X. Gigandet, P. Thiran, V. Wedeen, O. Sporns, C. Honey, R. Kotter, C. Stam, C. Stam, B. Jones, I. Manshanden, A. van C. van Walsum, T. Montez, D. Bassett, E. Bullmore, R. Ferri, F. Rundo, O. Bruni, M. Terzano, C. Stam, S. Achard, R. Salvador, B. Whitcher, J. Suckling, E. Bullmore, G. Tononi, G. Edelman, J. Damoiseaux, S. Rombouts, F. Barkhof, P. Scheltens, C. Stam, Y. Liu, M. Liang, Y. Zhou, Y. He, Y. Hao, S. Micheloyannis, E. Pachou, C. Stam, M. Breakspear, P. Bitsios, C. Stam, W. de Haan, A. Daffertshofer, B. Jones, I. Manshanden, H. Wang, T. Cui, F. Hou, Z. Ni, X. Chen, M. Folstein, S. Folstein, P. McHugh, G. McKhann, D. Drachman, M. Folstein, R. Katzman, D. Price, F. Fazekas, J. Chawluk, A. Alavi, H. Hurtig, R. Zimmerman, S. Smith, M. Jenkinson, M. Woolrich, C. Beckmann, T. Behrens, M. Jenkinson, P. Bannister, M. Brady, S. Smith, S. Smith, N. Tzourio-Mazoyer, B. Landeau, D. Papathanassiou, F. Crivello, O. Etard, T. Montez, K. Linkenkaer-Hansen, B. van Dijk, C. Stam, M. Newman, S. Ponten, F. Bartolomei, C. Stam, S. Maslov, K. Sneppen, E. Maris, R. Oostenveld, V. Eguiluz, D. Chialvo, G. Cecchi, M. Baliki, A. Apkarian, M. Kaiser, M. Kaiser, C. Hilgetag, L. Lago-Fernandez, R. Huerta, F. Corbacho, J. Siguenza, O. Sporns, D. Chialvo, M. Kaiser, C. Hilgetag, O. Sporns, G. Tononi, G. Edelman, C. Sorg, V. Riedl, M. Muhlau, V. Calhoun, T. Eichele, C. Grady, M. Furey, P. Pietrini, B. Horwitz, S. Rapoport, B. Horwitz, A. McIntosh, J. Haxby, M. Furey, J. Salerno, J. Hao, K. Li, D. Zhang, W. Wang, Y. Yang, Y. He, L. Wang, Y. Zang, L. Tian, X. Zhang, D. Prvulovic, D. Hubl, A. Sack, L. Melillo, K. Maurer, D. Alsop, J. Detre, M. Grossman, R. Buckner, A. Snyder, B. Shannon, G. LaRossa, R. Sachs, C. Lustig, A. Snyder, M. Bhakta, K. O'Brien, M. McAvoy, G. Karas, E. Burton, S. Rombouts, R. van Schijndel, J. O'Brien, G. Fein, V. Di Sclafani, J. Tanabe, V. Cardenas, M. Weiner, F. Block, M. Dihne, M. Loos, N. Villain, B. Desgranges, F. Viader, V. de la Sayette, F. Mezenge, C. Honey, O. Sporns, K. Friston, F. de Leeuw, F. Barkhof, P. Scheltens, J. Whitwell, S. Przybelski, S. Weigand, D. Knopman and B. Boeve, Loss of "Small-World" Networks in Alzheimer's Disease: Graph Analysis of fMRI Resting-State Functional Connectivity, *PLoS One* **5** (2010) e13788, doi:10.1371/journal.pone.0013788.

72. M. Ahmadlou, A. Adeli, R. Bajo and H. Adeli, Complexity of functional connectivity networks in mild cognitive impairment subjects during a working memory task, *Clin. Neurophysiol.* **125** (2014) 694–702, doi:10.1016/j.clinph.2013.08.033.

73. R. Salvador, J. Suckling, M. R. Coleman, J. D. Pickard, D. Menon and E. Bullmore, Neurophysiological Architecture of Functional Magnetic Resonance Images of Human Brain, *Cereb. Cortex* **15** (2004) 1332–1342, doi:10.1093/cercor/bhi016.

74. K. Supekar, V. Menon, D. Rubin, M. Musen and M. D. Greicius, Network Analysis of Intrinsic Functional Brain Connectivity in Alzheimer's Disease, *PLoS Comput. Biol.* **4** (2008) e1000100, doi:10.1371/journal.pcbi.1000100.

75. A. Ortiz, J. Munilla, I. Álvarez-Illán, J. M. Górriz and J. Ramírez, A.D.N. Alzheimer's Disease Neuroimaging Initiative, Exploratory graphical models of functional and structural connectivity patterns for Alzheimer's Disease diagnosis, *Front. Comput. Neurosci.* **9** (2015) 132, doi:10.3389/fncom.2015.00132.

76. J. Munilla, A. Ortiz, J. M. Górriz and J. Ramírez, the A.D.N. Alzheimer's Disease Neuroimaging Initiative, Construction and Analysis of Weighted Brain Networks from SICE for the Study of Alzheimer's Disease, *Front. Neuroinform.* **11** (2017) 19, doi:10.3389/fninf.2017.00019.

77. H.-C. Baggio, R. Sala-Llonch, B. Segura, M.-J. Marti, F. Valldeoriola, Y. Compta, E. Tolosa and C. Junqué, Functional brain networks and cognitive deficits in Parkinson's disease, *Hum. Brain Map.* **35** (2014) 4620–4634, doi:10.1002/hbm.22499.

78. W. de Haan, W. M. van der Flier, T. Koene, L. L. Smits, P. Scheltens and C. J. Stam, Disrupted modular brain dynamics reflect cognitive dysfunction in Alzheimer's disease, *Neuroimage* **59** (2012) 3085–3093, doi:10.1016/j.neuroimage.2011.11.055.

79. M. G. Kitzbichler, R. N. A. Henson, M. L. Smith, P. J. Nathan and E. T. Bullmore, Cognitive Effort Drives Workspace Configuration of Human Brain Functional Networks, *J. Neurosci.* **31** (2011).

80. D. T. Jones, M. M. Machulda, P. Vemuri, E. M. McDade, G. Zeng, M. L. Senjem, J. L. Gunter, S. A.

Przybelski, R. T. Avula, D. S. Knopman, B. F. Boeve, R. C. Petersen and C. R. Jack, Age-related changes in the default mode network are more advanced in Alzheimer disease, *Neurology* **77** (2011) 1524–1531, doi:10.1212/WNL.0b013e318233b33d.

81. M. Yu, A. A. Gouw, A. Hillebrand, B. M. Tijms, C. J. Stam, E. C. W. van Straaten and Y. A. L. Pijnenburg, Different functional connectivity and network topology in behavioral variant of frontotemporal dementia and Alzheimer's disease: An EEG study, *Neurobiol. Aging* **42** (2016) 150–162, doi:10.1016/j.neurobiolaging.2016.03.018.
82. M. M. A. Engels, C. J. Stam, W. M. van der Flier, P. Scheltens, H. de Waal and E. C. W. van Straaten, Declining functional connectivity and changing hub locations in Alzheimer's disease: an EEG study., *BMC Neurol.* **15** (2015) 145, doi:10.1186/s12883-015-0400-7.
83. S. Huang, J. Li, L. Sun, J. Ye, A. Fleisher, T. Wu, K. Chen and E. Reiman, Learning brain connectivity of Alzheimer's disease by sparse inverse covariance estimation, *Neuroimage* **50** (2010) 935–949, doi:10.1016/j.neuroimage.2009.12.120.
84. D. López-Sanz, R. Bruña, P. Garcés, M. C. Martín-Buro, S. Walter, M. L. Delgado, M. Montenegro, R. López Higes, A. Marcos and F. Maestú, Functional Connectivity Disruption in Subjective Cognitive Decline and Mild Cognitive Impairment: A Common Pattern of Alterations, *Front. Aging Neurosci.* **9** (2017) 109, doi:10.3389/fnagi.2017.00109.
85. R. Albert, H. Jeong and A.-L. Barabási, Error and attack tolerance of complex networks, *Nature* **406** (2000) 378–382, doi:10.1038/35019019.
86. J. M. Buldú, R. Bajo, F. Maestú, N. Castellanos, I. Leyva, P. Gil, I. Sendiña-Nadal, J. A. Almendral, A. Nevado, F. del-Pozo, S. Boccaletti, J. Palva, S. Monto, S. Kulashekhar, S. Palva, M. Newman, S. Boccaletti, V. Latora, Y. Moreno, M. Chavez, D. Hwang, M. Rubinov, O. Sporns, C. van Leeuwen, M. Breakspear, D. Watts, S. Strogatz, C. Stam, W. de Haan, A. Daffertshofer, B. Jones, I. Manshanden, X. Delbeuck, M. Van der Linden, F. Collette, C. Stam, B. Jones, G. Nolte, M. Breakspear, P. Scheltens, K. Supekar, V. Menon, D. Rubin, M. Musen, M. Greicius, H. Braak, E. Braak, R. Petersen, W. Markesbery, B. Dickerson, D. Salat, D. Greve, E. Chua, E. Rand-Giovannetti, R. Bajo, F. Maestú, A. Nevado, M. Sancho, R. Gutiérrez, L. deToledo-Morrell, S. Evers, T. Hoeppner, F. Morrell, D. Garron, F. Maestu, A. Fernandez, P. Simos, P. Gil-Gregorio, C. Amo, C. Stam, C. Babiloni, R. Ferri, G. Binetti, A. Cassarino, G. D. Forno, D. Meunier, S. Achard, A. Morcom, E. Bullmore, S. Ahnert, D. Garlaschelli, T. Fink, G. Caldarelli, E. Dijkstra, M. Newman, M. Girvan, M. Newman, V. Eguíluz, D. Chialvo, G. Cecchi, M. Baliki, A. Apkarian, A. Holmes, R. Blair, J. Watson, I. Ford, T. Nichols, A. Holmes, M. Ernst, O. Sporns, G. Tononi, G. Edelman, R. Guimera, L. N. Amaral, Y. He, Z. Chen, A. Evans, J. Schneider, Z. Arvanitakis, S. Leurgans, D. Bennett, S. Scheff, D. Price, F. Schmitt, S. DeKosky, E. Mufson, J. Sepulcre, H. Liu, T. Talukdar, I. Martincorena, B. Yeo, S. Achard, E. Bullmore, D. Fair, A. Cohen, J. Power, N. Dosenbach, J. Church, M. Corbetta, G. Shulman, M. Chun, N. Turk-Browne and D. Drachman, Reorganization of Functional Networks in Mild Cognitive Impairment, *PLoS One* **6** (2011) e19584, doi:10.1371/journal.pone.0019584.
87. A. Maass, S. Landau, S. L. Baker, A. Horng, S. N. Lockhart, R. La Joie, G. D. Rabinovici and W. J. Jagust, Comparison of multiple tau-PET measures as biomarkers in aging and Alzheimer's disease, *Neuroimage.* **157** (2017) 448–463, doi:10.1016/j.neuroimage.2017.05.058.
88. A. Perrotin, R. de Flores, F. Lamberton, G. Poisnel, R. La Joie, V. de la Sayette, F. Mézenge, C. Tomadesso, B. Landeau, B. Desgranges and G. Chételat, Hippocampal Subfield Volumetry and 3D Surface Mapping in Subjective Cognitive Decline, *J. Alzheimer's Dis.* **48** (2015) S141–S150, doi:10.3233/JAD-150087.
89. R. Tepest, L. Wang, J. G. Csernansky, P. Neubert, R. Heun, L. Scheef and F. Jessen, Hippocampal surface analysis in subjective memory impairment, mild cognitive impairment and Alzheimer's dementia, *Dement. Geriatr. Cogn. Disord.* **26** (2008) 323–329, doi:10.1159/000161057.
90. Q. Zhou, M. Goryawala, M. Cabrerizo, J. Wang, W. Barker, D. A. Loewenstein, R. Duara and M. Adjouadi, An Optimal Decisional Space for the Classification of Alzheimer's Disease and Mild Cognitive Impairment, *IEEE Trans. Biomed. Eng.* **61** (2014) 2245–2253, doi:10.1109/TBME.2014.2310709.
91. J. Peter, L. Scheef, A. Abdulkadir, H. Boecker, M. Heneka, M. Wagner, A. Koppara, S. Klöppel and F. Jessen, Gray matter atrophy pattern in elderly with subjective memory impairment, *Alzheimer's Dement.* **10** (2014) 99–108, doi:10.1016/j.jalz.2013.05.1764.
92. N. Striepens, L. Scheef, A. Wind, J. Popp, A. Spottke, D. Cooper-Mahkorn, H. Suliman, M. Wagner, H. H. Schild and F. Jessen, Volume Loss of the Medial Temporal Lobe Structures in Subjective Memory Impairment, *Dement. Geriatr. Cogn. Disord.* **29** (2010) 75–81, doi:10.1159/000264630.
93. A. Perrotin, E. C. Mormino, C. M. Madison, A. O. Hayenga and W. J. Jagust, Subjective cognition and amyloid deposition imaging: a Pittsburgh Compound B positron emission tomography study in normal elderly individuals., *Arch. Neurol.* **69** (2012) 223–229, doi:10.1001/archneurol.2011.666.

94. B. E. Snitz, L. A. Weissfeld, A. D. Cohen, O. L. Lopez, R. D. Nebes, H. J. Aizenstein, E. McDade, J. C. Price, C. A. Mathis and W. E. Klunk, Subjective cognitive complaints, personality and brain amyloid-beta in cognitively normal older adults, *Am. J. Geriatr. Psychiatry.* **23** (2015) 985–993, doi:10.1016/j.jagp.2015.01.008.
95. R. Duara, W. Barker, D. Loewenstein, M. T. Greig, R. Rodriguez, M. Goryawala, Q. Zhou and M. Adjouadi, Insights into cognitive aging and Alzheimer's disease using amyloid PET and structural MRI scans, *Clin. Transl. Imag.* **3** (2015) 65–74, doi:10.1007/s40336-015-0110-6.
96. P. J. Visser, F. Verhey, D. L. Knol, P. Scheltens, L.-O. Wahlund, Y. Freund-Levi, M. Tsolaki, L. Minthon, A. K. Wallin, H. Hampel, K. Bürger, T. Pirttila, H. Soininen, M. O. Rikkert, M. M. Verbeek, L. Spiru and K. Blennow, Prevalence and prognostic value of CSF markers of Alzheimer's disease pathology in patients with subjective cognitive impairment or mild cognitive impairment in the DESCRIPA study: a prospective cohort study, *Lancet. Neurol.* **8** (2009) 619–627, doi:10.1016/S1474-4422(09)70139-5.
97. F. J. Martinez-Murcia, J. M. Gorriz, J. Ramirez and A. Ortiz, A Structural Parametrization of the Brain Using Hidden Markov Models-Based Paths in Alzheimer's Disease, *Int. J. Neural Syst.* **26** (2016) 1650024, doi:10.1142/S0129065716500246.
98. A. Ortiz, J. Munilla, J. M. Górriz and J. Ramírez, Ensembles of Deep Learning Architectures for the Early Diagnosis of the Alzheimer's Disease, *Int. J. Neural Syst.* **26** (2016) 1650025, doi:10.1142/S0129065716500258.
99. F. J. Martinez-Murcia, J. M. Gorriz, J. Ramirez and A. Ortiz, I. For The Alzheimer's Disease Neuroimaging, A Spherical Brain Mapping of MR Images for the Detection of Alzheimer's Disease, *Curr Alzheimer Res.* **13** (2016) 575–588, http://www.ingentaconnect.com/contentone/ben/car/2016/00000013/00000005/art00012 (accessed on 7 June, 2017).
100. J. P. Amezquita-Sanchez, A. Adeli and H. Adeli, A new methodology for automated diagnosis of mild cognitive impairment (MCI) using magnetoencephalography (MEG), *Behav. Brain Res.* **305** (2016) 174–180, doi:10.1016/j.bbr.2016.02.035.
101. M. E. López, R. Bruña, S. Aurtenetxe, J. A. Pineda-Pardo, A. Marcos, J. Arrazola, A. I. Reinoso, P. Montejo, R. Bajo and F. Maestú, Alpha-band hypersynchronization in progressive mild cognitive impairment: a magnetoencephalography study, *J. Neurosci.* **34** (2014) 14551–14559, doi:10.1523/JNEUROSCI.0964-14.2014.
102. G. Mirzaei, A. Adeli and H. Adeli, Imaging and machine learning techniques for diagnosis of Alzheimer's disease, *Rev. Neurosci.* **27** (2016) 857–870, doi:10.1515/revneuro-2016-0029.